Deformation dependence of the isovector giant dipole resonance: The neodymium isotopic chain revisited

L.M. Donaldson[a], C.A. Bertulani[g], J. Carter[a], V.O. Nesterenko[b], P. von Neumann-Cosel[c,*], R. Neveling[d], P.-G. Reinhard[e], I.T. Usman[a], P. Adsley[d,f], J.W. Brummer[f], E.Z. Buthelezi[d], G.R.J. Cooper[h], R.W. Fearick[i], S.V. Förtsch[d], H. Fujita[j], Y. Fujita[k], M. Jingo[a], W. Kleinig[b], C.O. Kureba[a], J. Kvasil[l], M. Latif[a], K.C.W. Li[f], J.P. Mira[d], F. Nemulodi[d], P. Papka[d,f], L. Pellegri[a,d], N. Pietralla[c], A. Richter[c], E. Sideras-Haddad[a], F.D. Smit[d], G.F. Steyn[d], J.A. Swartz[f], A. Tamii[j]

[a] *School of Physics, University of the Witwatersrand, Johannesburg 2050, South Africa*
[b] *Bogoliubov Laboratory of Theoretical Physics, Joint Institute for Nuclear Research, Dubna, Moscow region, 141980, Russia*
[c] *Institut für Kernphysik, Technische Universität Darmstadt, D-64289 Darmstadt, Germany*
[d] *iThemba LABS, P. O. Box 722, Somerset West 7129, South Africa*
[e] *Institut für Theoretische Physik II, Universität Erlangen, D-91058 Erlangen, Germany*
[f] *Department of Physics, University of Stellenbosch, Matieland 7602, South Africa*
[g] *Department of Physics and Astronomy, Texas A&M University-Commerce, Commerce, Texas 75429, USA*
[h] *School of Geosciences, University of the Witwatersrand, Johannesburg 2050, South Africa*
[i] *Department of Physics, University of Cape Town, Rondebosch 7700, South Africa*
[j] *Research Center for Nuclear Physics, Osaka University, Ibaraki, Osaka 567-0047, Japan*
[k] *Department of Physics, Osaka University, Toyonaka, Osaka 560-0043, Japan*
[l] *Institute of Particle and Nuclear Physics, Charles University, CZ-18000, Prague 8, Czech Republic*

Abstract

Proton inelastic scattering experiments at energy $E_{\mathrm{p}} = 200\,\mathrm{MeV}$ and a spectrometer scattering angle of 0° were performed on ^{144,146,148,150}Nd and ^{152}Sm exciting the IsoVector Giant Dipole Resonance (IVGDR). Comparison with results from photo-absorption experiments reveals a shift of resonance maxima towards higher energies for vibrational and transitional nuclei. The most deformed nuclei, ^{150}Nd and ^{152}Sm, lack the double-hump structure previously observed in photo-absorption experiments and interpreted as a signature of K-splitting. Self-consistent random-phase approximation (RPA) calculations using the SLy6 Skyrme force provide a good description of the data from the present experiments.

Keywords: ^{144,146,148,150}Nd, ^{152}Sm(p,p′), $E_{\mathrm{p}} = 200$ MeV, $\theta_{\mathrm{lab}} = 0^\circ$, relativistic Coulomb excitation of the IVGDR, comparison with photo-absorption results, transition from spherical to deformed nuclei

1. Introduction

Giant resonances represent a prime example of collective modes in the nucleus. A smooth mass-number dependence of the resonance parameters is characteristic of all nuclear giant resonances and, as such, a study of them yields information about the non-equilibrium dynamics and the bulk properties of the nucleus [1]. The oldest and best known giant resonance is the IVGDR owing to the high selectivity for isovector E1 excitation in photo-absorption experiments. The properties of the IVGDR have been studied extensively using (γ,xn)-type experiments, particularly in the Saclay [2] and Livermore [3] laboratories. These sets of experiments are a major source of information with respect to the γ-strength function [4] above the neutron threshold - an important quantity used in statistical reaction calculations relevant to applications like astrophysical large-scale reaction networks [5, 6], reactor design [7], or nuclear waste transmutation [8].

Recently, a new experimental technique for the extraction of electric dipole-strength distributions in nuclei via relativistic Coulomb excitation has been developed [9, 10]. It utilises proton inelastic scattering with energies of a few hundred MeV

*Corresponding author
Email addresses: lindsay.donaldson18@gmail.com (L.M. Donaldson), vnc@ikp.tu-darmstadt.de (P. von Neumann-Cosel)

at scattering angles close to 0°. Although many experiments focus on establishing the strength below the neutron threshold and its contribution to the dipole polarizability [11–14], such data also provide information on the photo-absorption cross sections in the energy region of the IVGDR.

The chain of stable even-even neodymium isotopes is known to comprise a sudden transition from spherical to deformed ground states for heavier isotopes and thus represents an excellent test case to study the influence of deformation on the properties of the IVGDR. A (γ,xn) experiment at Saclay [15] revealed that the width increases with deformation evolving into a pronounced double-hump structure in the most deformed nuclide ^{150}Nd, considered to be a textbook example [16] of K-splitting owing to oscillations along the different axes of the quadrupole-deformed ground state. Here, we report new photo-absorption cross sections for ^{144,146,148,150}Nd extracted from 200 MeV proton scattering experiments with results differing significantly from Ref. [15]. In particular, no double-hump structure is observed in the most deformed ^{150}Nd nucleus. This finding is confirmed in a further measurement of the comparably deformed ^{152}Sm nucleus, again in contrast to (γ,xn) results [17]. This unexpected result may be related to the special structure of these two nuclei which are predicted to lie near the critical point of a shape phase transition from spherical to quadrupole-deformed ground states.

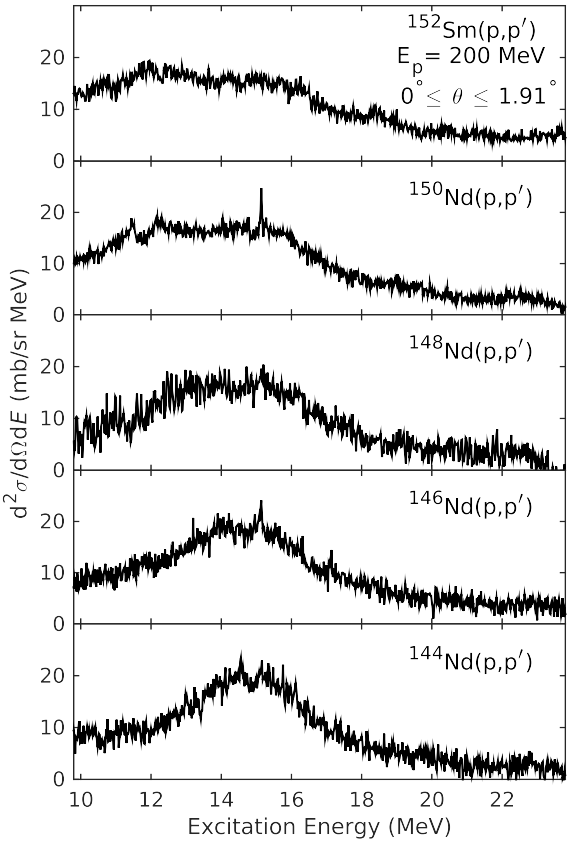

Figure 1: Experimental double-differential cross sections for the ^{144,146,148,150}Nd(p,p′) and ^{152}Sm(p,p′) reactions at $E_{\rm p} = 200$ MeV and $\theta_{\rm Lab} = 0° - 1.91°$.

2. Experiment and analysis

The proton inelastic scattering experiments were performed at the iThemba Laboratory for Accelerator Based Sciences (iThemba LABS) in South Africa. The K600 magnetic spectrometer, positioned at 0° with the acceptance defined by a circular collimator having an opening angle $\theta_{\rm lab} = \pm 1.91°$, was used to analyse a 200 MeV dispersion-matched proton beam delivered from the Separated Sector Cyclotron of iThemba LABS. The self-supporting ^{144,146,148,150}Nd and ^{152}Sm targets were all isotopically enriched to values >96% (except ^{148}Nd enriched to 90%) with areal densities ranging from 1.8 to 2.6 mg/cm^2. The corresponding ground-state deformation parameters β_2 are given in the second column of Table 1. The beam preparation and the detector setup are described in Ref. [10]. Details regarding the data extraction and analysis of the present measurements can be found in Ref. [18].

In the chosen kinematic conditions, relativistic Coulomb excitation is the dominant reaction mechanism. The resulting double differential cross sections obtained following the procedures detailed in Ref. [18] are displayed in Fig. 1 for 20 keV energy bins. A typical energy resolution $\Delta E = 45$ keV (FWHM) was achieved with a systematic uncertainty of the cross sections amounting to ±7%. The broad structure visible in all spectra between approximately $E_{\rm x} = 12$ and 18 MeV corresponds to the excitation of the IVGDR. Statistical errors in this region are 2-4%. The sharp peak at $E_{\rm x} \approx 15$ MeV visible in some spectra results from the M1 transition in ^{12}C to a state at $E_{\rm x} = 15.11$ MeV [19] prominently excited in the (p,p′) reaction at small momentum transfers. From Fig. 1 it is immedi-

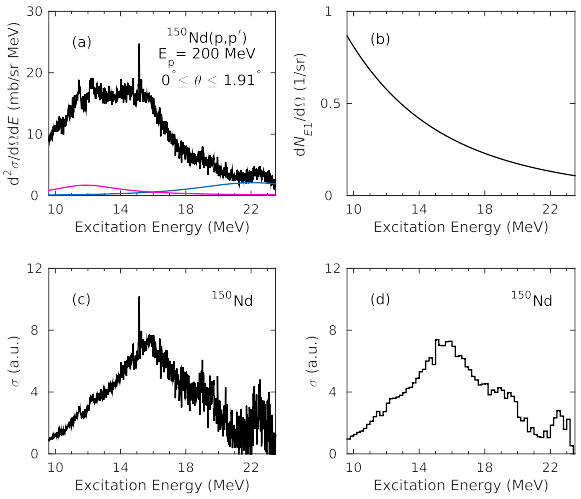

Figure 2: (Colour online). Overview of the conversion process from ^{150}Nd(p,p′) to photo-absorption cross sections: (a) double-differential (p,p′) cross section and background components. The pink line describes the contribution from the ISGQR and the blue line the phenomenological component explained in the text; (b) virtual photon spectrum; (c) equivalent photo-absorption spectrum resulting from Eq. (1); (d) equivalent photo-absorption spectrum rebinned to 200 keV for comparison with photo-absorption data [15].

ately clear that the width of the IVGDR increases steadily from the nearly spherical ^{144}Nd nucleus through the transition region to the more deformed ^{150}Nd and ^{152}Sm nuclei.

In order to compare to the (γ,xn) data of Carlos et al. [15, 17], the (p,p′) spectra had to be converted to equivalent photo-absorption cross sections. By way of example, Fig. 2 provides an overview of the conversion process for the ^{150}Nd isotope. It can be divided into three distinct stages, namely, background subtraction in the region of the IVGDR, calculation of the virtual-photon spectrum and the division by this spectrum multiplied through by the vitual γ energy to obtain equivalent photo-absorption cross sections.

Background from nuclear processes studied in similar experiments at 300 MeV has been found to be small [11–14]. The background to the measured spectra was modelled by two Lorentzian components. The contribution of the IsoScalar Giant Quadrupole Resonance (ISGQR) to the spectrum of Fig. 2(a) (pink line) was determined through the use of position and width information from a study of the ISGQR in the Nd isotope chain [20] with methods analogous to Refs. [21–23]. The strength of the ISGQR contribution was estimated from the ratio of GQR strength to GDR strength as provided from Distorted Wave Born Approximation (DWBA) calculations assuming 100 % exhaustion of the energy-weighted sum rule.

A phenomenological background (blue line) describes the behaviour of the double-differential cross section at the high excitation energy part of the spectrum where the Coulomb excitation contribution to the cross section is negligible. This component incorporates all unknown multipolarity contributions as well as quasi-free scattering and is approximated by finding the maximum of the cross section between $E_x = 20$ MeV and 23 MeV and using a width that best describes the spectrum in this region. A similar description for the shape of this component was found in a study of ^{208}Pb with the same method [24] where an experimental extraction of the angular distribution of the background was possible.

The virtual E1 photon spectrum [25] for each isotope was calculated using the eikonal approximation [26] and averaged over the angular acceptance of the detector. The equivalent photo-absorption spectrum (cf. Fig. 2(c)) was then obtained using the following equation

$$\frac{d^2\sigma}{d\Omega dE_\gamma} = \frac{1}{E_\gamma}\frac{dN_{E1}}{d\Omega}\sigma_\gamma^{\pi\lambda}(E_\gamma). \qquad (1)$$

Finally, Fig. 2(d) shows the equivalent photo-absorption spectrum rebinned to 200 keV for direct comparison with the (γ,xn) results. The present setup at $\theta_{\rm lab} = 0°$ does not allow for the determination of accurate vertical scattering angles, thus limiting the angular resolution [10]. We therefore refrain from extracting absolute photo-absorption cross sections. The excitation energy dependence of the conversion, however, is not affected.

3. Comparison with (γ,xn) results

Through the simultaneous measurement of the partial photo-nuclear cross sections $\sigma(\gamma, \mathrm{n}) + \sigma(\gamma, \mathrm{pn})$ and $\sigma(\gamma, 2\mathrm{n})$ using a monochromatic photon beam total photo-absorption cross sections can be determined in heavy nuclei. Data obtained with this method for the IVGDR in the stable even-even neodymium and samarium isotopic chains are given in Refs. [15] and [17], respectively. Figure 3 displays the rebinned spectra from the present work normalised to the photo-absorption cross sections [15, 17] to facilitate a comparison of the evo-

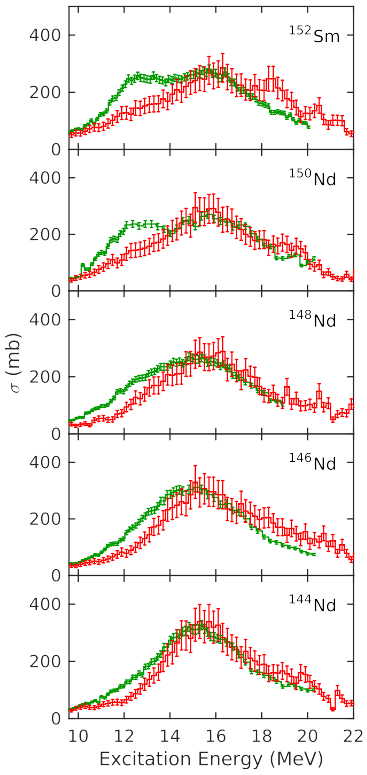

Figure 3: (Colour online). Comparison between the normalised ^{144,146,148,150}Nd and ^{152}Sm photo-absoprtion cross sections derived from the present data (red histograms) and the pre-existing (γ,xn) results (green histograms) [15, 17].

lution of the shape of the IVGDR with increasing deformation.

Carlos et al. [15, 17] (green histograms) observed a spreading of the IVGDR as the nuclei become softer followed by a splitting of the IVGDR into two distinct dipole modes for ^{150}Nd and ^{152}Sm, which were interpreted as $K = 0$ and $K = 1$ components. The equivalent photo-absorption cross sections from the present work (red histograms) display a similar trend, i.e., a general broadening of the IVGDR with increasing deformation. For the most deformed ^{150}Nd and ^{152}Sm, the resonance becomes skewed with enhanced strength on the low-energy side, but no split into two distinct components is observed.

The obvious discrepancies (in both the $K = 0$ and $K = 1$ regions) between the photo-absorption results and the present data are reflected in a change of parameters when attempting to describe the observed resonances by Lorentzians. The present spectra were fitted with a modified Lorentzian of the form used in Refs. [15, 17],

$$\sigma(E) = \frac{\sigma_{\rm R}}{1 + [(E^2 - {E_{\rm R}}^2)^2/E^2\Gamma^2]} \ , \qquad (2)$$

where $\sigma_{\rm R}$ corresponds to the maximum of the resonance, $E_{\rm R}$ to the resonance centroid energy and $\Gamma_{\rm R}$ to the resonance half-width. For the more deformed nuclei, a sum of two modified Lorentzians was used. The best fit to the experimental data was selected such that the value for the reduced χ^2 was optimised. In the case of the ^{148}Nd isotope, it was found that the reduced χ^2 value was not improved through the use of a two Lorentzian fit as assumed in a reanalysis [27] of the data of Ref. [15].

The parametrisations obtained in the present study together with those from Carlos et al. [15, 17] are presented in Table 1. For spherical and transitional nuclei, a shift of the centroid to higher energies is observed for the present data. The new parametrisations for the deformed nuclei do not yield a ratio of ≈ 0.5 for $K = 0$ and $K = 1$ oscillator strengths, respectively, as expected for prolate deformed ground states [3]. One should remember, however, that ^{150}Nd and ^{152}Sm lie just above the shape phase transition from vibrators to axial rotors [28, 29]. Although they are already well deformed, their deformation potential is soft in the β degree of freedom [30]. The corresponding shape fluctuations thus enhance the width of the resonance peaks which, in turn, may hinder a clear discrimination of the $K = 0$ and 1 branches.

As can be seen from Fig. 3 and Table 1, the most obvious discrepancies are found in the lower excitation-energy ($K = 0$) region. When normalised to facilitate a shape comparison between the two data sets, the contributions to the equivalent photo-absorption cross sections in the $K = 0$ region are substantially lower than those reported by Carlos et al. [15, 17]. Recent (γ,n) experiments [31, 32] also find systematically smaller photo-absorption cross sections in the excitation-energy region between the neutron threshold and $E_{\rm x} \approx 13$ MeV corroborating the present results. Furthermore, a recent study of the E1 strength in ^{154}Sm [33] with the methods decribed in Refs. [11–14] does find a double-hump structure but with a clearly reduced $K = 0/K = 1$ ratio compared to the Saclay data [17]. These findings are qualitatively consistent with a reanalysis of the Saclay method [34], which indicates that their (γ,n) cross sections are too large and (γ,2n) cross sections too small.

Table 1: Comparison of Lorentzian parameterisations, Eq. (2), for the present photo-absorption cross sections with those from Ref. [15] for the neodymium isotopes and from Ref. [17] for ^{152}Sm.

Isotope	β_2 [39]	E_1 (MeV)	σ_1 (mb)	Γ_1 (MeV)	E_2 (MeV)	σ_2 (mb)	Γ_2 (MeV)	Reference
^{144}Nd	0.13	15.05±0.10	317±15	5.30±0.25				[15]
		15.64±0.01		4.93±0.03				Present
^{146}Nd	0.15	14.80±0.10	308±16	6.00±0.30				[15]
		15.69±0.02		6.11±0.07				Present
^{148}Nd	0.20	14.70±0.15	263±15	7.20±0.30				[15]
		15.52±0.01		5.84±0.04				Present
^{150}Nd	0.28	12.30±0.15	174±20	3.30±0.10	16.00±0.15	223±20	5.20±0.15	[15]
		11.97±0.10		2.91±0.40	15.67±0.04		5.64±0.09	Present
^{152}Sm	0.31	12.45±0.10	183±10	3.20±0.15	15.85±0.10	226±10	5.10±0.20	[17]
		12.40±0.20		4.73±0.65	16.36±0.07		6.36±0.14	Present

4. Comparison with model calculations

In order to investigate the role of $K = 0$ and $K = 1$ components further, a comparison with RPA calculations particularly suited for modelling the IVGDR is presented. The calculations are performed within the Skyrme Separable Random Phase Approximation (SSRPA) approach [35]. The method is fully self-consistent since both the mean field and residual interaction are derived from the same Skyrme functional. The residual interaction includes all the functional contributions as well as the Coulomb direct and exchange terms. The self-consistent factorisation of the residual interaction crucially reduces the computational effort for deformed nuclei and maintains high accuracy of the calculations [35–37].

The Skyrme parameterisation SLy6 [38] is used, which was shown to be optimal for the description of the IVGDR in medium-heavy, deformed nuclei [37]. The code exploits the 2D grid in cylindrical coordinates. Usually, the axial quadrupole deformation characterised by the parameter β_2 is determined by minimisation of the total energy, and β_2 values obtained are typically close to experiment [37]. Nd and Sm isotopes in the transitional region, however, show very soft deformation energy surfaces, which gives a large uncertainty to the theoretical ground-state deformations. We thus adopt the experimental values $\beta_2 = 0.15$, 0.20, 0.29 and 0.31 [39] for the quadrupole deformation in ^{146,148,150}Nd and ^{152}Sm, respectively. For the nearly spherical ^{144}Nd, a negligible deformation, $\beta_2 = 0.001$, is used. Pairing is treated with delta forces at the BCS level [40]. A large two-quasiparticle basis up to $\sim$100 MeV is taken into account. The energy-weighted sum rule for isovector E1 strength is exhausted by $98 - 100\%$. The SSRPA strength function $S(\mathrm{E1})(E) = \sum_i E_i \mathrm{B(E1)}_i \xi_D(E - E_i)$ (sum over all SSRPA states) uses a Lorentz folding ξ_D with an averaging parameter $D = 2$ keV.

To facilitate a broad structure comparison between the experimental results and the model calculations, the SSRPA predictions were smoothed with a large width $\Gamma = 2$ MeV. The resulting photo-absorption cross sections are shown in Fig. 4 as green ($K = 0$), blue ($K = 1$) and red (total) lines. When the experimental data are normalised to exhaust the theoretically predicted energy-weighted sum rules, good agreement is obtained. For ^{150}Nd and ^{152}Sm, the $K = 0$ component overshoots the data (but lies below the Saclay results). It is clear from the above arguments that the assumption of a ground state with a well-defined prolate quadrupole deformation underlying the calculations is questionable for these nuclei.

5. Conclusions

A measurement of the (p,p′) reaction at $E_\mathrm{p} = 200$ MeV and $\theta = 0°$ favouring relativistic Coulomb excitation in the energy region of the IVGDR has been presented for the even-even $^{144-150}$Nd isotopic chain as well as for ^{152}Sm. While the high energy-resolution data show considerable fine structure (even in the deformed isotopes), which carries information on the role of different decay mecha-

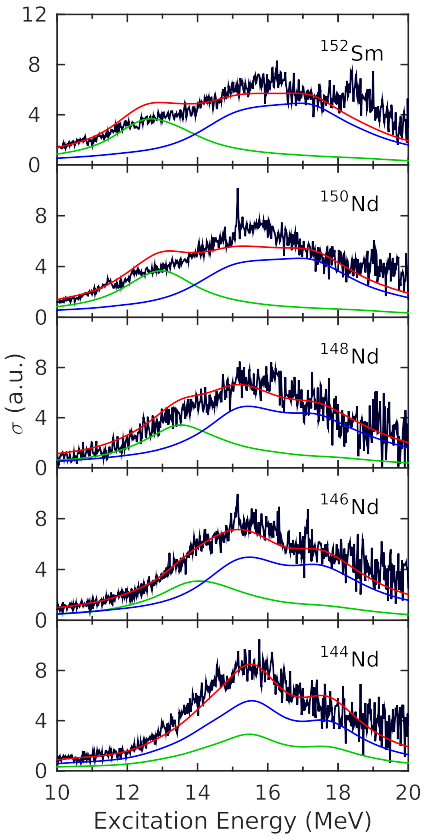

Figure 4: (Colour online). Comparison of the equivalent photo-absorption spectra from the present work and the SS-RPA predictions smoothed to a width of 2 MeV.

nisms of the giant resonances [21–24] and level densities [24, 41], the present work focuses on a study of the evolution of the IVGDR as a function of deformation.

A general broadening of the IVGDR is observed with increasing deformation and the most deformed ^{150}Nd and ^{152}Sm nuclei exhibit a prononounced asymmetry, but no double-hump structure owing to K-splitting evolves in contrast to previous photo-absorption data from Saclay [15, 17]. This is interpreted as a signature of the peculiar nature of these two nuclei which lie close to the critical point of a shape phase transition from vibrators to rotators characterised by a soft potential in β [30]. Self-consistent RPA model calculations with the Skyrme SLy6 force particularly suited to describe the IVGDR provide a fair description of the data consistent with the reduction of cross sections on the low-energy side of the resonance with respect to the Saclay data observed in recent experiments [31, 32] and suggested by a reanalysis [34]. In view of their general relevance, the present results call for a systematic reinvestigation of photo-absorption data in heavy deformed nuclei.

Acknowledgements

We thank J.L. Conradie and the accelerator team at iThemba LABS for providing excellent beams. Useful discussions with V.Yu. Ponomarev are gratefully acknowledged. This work was supported by the South African NRF and the DFG under contract No. SFB 1245. C.A.B. acknowledges support by the U.S. DOE grant DE-FG02-08ER41533 and the U.S. NSF Grant No. 1415656 and J.K. by the Czech Science Foundation (Grant No. P203-13-07117S).

References

[1] M.N. Harakeh, A. van der Woude, Giant Resonances: Fundamental High-Frequency Modes of Nuclear Excitation (Oxford University Press, Oxford, 2001).
[2] R. Bergère, Lecture Notes in Physics 61 (Springer, Berlin-Heidelberg-New York, 1977) 1.
[3] B.L. Berman, S.C. Fultz, Rev. Mod. Phys. 47 (1975) 713.
[4] G.A. Bartholomew, et al., Adv. Nucl. Phys. 7 (1973) 229.
[5] M. Arnould, S. Goriely, K. Takahashi, Phys. Rep. 450 (2007) 97.
[6] F. Käppeler, R. Gallino, S. Bisterzo, Wako Aoki, Rev. Mod. Phys. 83 (2011) 157.
[7] M.B. Chadwick, et al., Nucl. Data Sheets 112 (2011) 2887.
[8] C.D. Bowman, Annu. Rev. Nucl. Part. Sci. 48 (1998) 505.
[9] A. Tamii, et al., Nucl. Instrum. Methods A 605 (2009) 326.
[10] R. Neveling, et al., Nucl. Instrum. Methods A 654 (2011) 29.
[11] A. Tamii, et al., Phys. Rev. Lett. 107 (2011) 062502.
[12] I. Poltoratska, et al., Phys. Rev. C 85 (2012) 041304(R).
[13] A.M. Krumbholz, et al., Phys. Lett. B 744 (2015) 7.
[14] T. Hashimoto, et al., Phys. Rev. C 92 (2015) 031305(R).
[15] P. Carlos, H. Beil, R. Bergère, A. Leprêtre, A. Veyssière, Nucl. Phys. A 172 (1971) 437.
[16] A. Bohr, B.R. Mottelson, Nuclear Structure Vol. II (Benjamin, Reading, 1975) p. 490 ff.
[17] P. Carlos, H. Beil, R. Bergère, A. Leprêtre, A. De Miniac, A. Veyssière, Nucl. Phys. A 225 (1974) 171.
[18] L.M. Donaldson, PhD thesis, University of the Witwatersrand (2016); and to be published.

[19] F. Ajzenberg-Selove, J.H. Kelley, Nucl. Phys. A 506 (1990) 1.
[20] C.O. Kureba, PhD thesis, University of the Witwatersrand (2014), and to be published.
[21] A. Shevchenko, et al., Phys. Rev. Lett. 93 (2004) 122501.
[22] A. Shevchenko, et al., Phys. Rev. C 79 (2009) 044305.
[23] I. Usman, et al., Phys. Lett. B 698 (2011) 191.
[24] I. Poltoratska, et al., Phys. Rev. C 89 (2014) 054322.
[25] C.A. Bertulani, G. Baur, Phys. Rep. 163 (1988) 299.
[26] C.A. Bertulani, A.M. Nathan, Nucl. Phys. A 554 (1993) 158.
[27] R. Capote, et al., Nucl. Data Sheets 110 (2009) 3107.
[28] R.F. Casten, N.V. Zamfir, Phys. Rev. Lett. 87 (2001) 052503.
[29] R.F. Casten, Nature Physics 2 (2006) 811.
[30] F. Iachello, Phys. Rev. Lett. 87 (2001) 052502.
[31] H.-T. Nyhus, et al., Phys. Rev. C 91 (2015) 015808.
[32] D.M. Filipescu, et al., Phys. Rev. C 90 (2014) 064616.
[33] A. Krugmann, D. Martin, P. von Neumann-Cosel, N. Pietralla, A. Tamii, EPJ Web of Conferences 66 (2014) 02060; and to be published.
[34] V.V. Varlamov, B.S. Ishkhanov, V.N. Orlin, K.A. Stopani, Eur. Phys. J. A 50 (2014) 114.
[35] V.O. Nesterenko, et al., Phys. Rev. C 74 (2006) 064306.
[36] V.O. Nesterenko, et al., Int. J. Mod. Phys. E 17 (2008) 89.
[37] W. Kleinig, V.O. Nesterenko, J. Kvasil, P.-G. Reinhard, P. Vesely, Phys. Rev. C 78 (2008) 044313.
[38] E. Chabanat, P. Bonche, P. Haensel, J. Meyer, R. Schaeffer, Nucl. Phys. A 635 (1998) 231.
[39] S. Raman, C.H. Malarkey, W.T. Milner, C.W. Nestor Jr., P.H. Stelson, At. Data Nucl. Data Tables 36 (1987) 1.
[40] M. Bender, K. Rutz, P.-G. Reinhard, J.A. Maruhn, Eur. Phys. J. A 8 (2000) 59.
[41] I. Usman, et al., Phys. Rev. C 84 (2011) 054322.